Disruption of *ldlr* causes increased LDL-c and vascular lipid accumulation in a zebrafish model of hypercholesterolemia[S]

Elizabeth A. O'Hare, Xiaochun Wang, May E. Montasser, Yen-Pei C. Chang, Braxton D. Mitchell, and Norann A. Zaghloul[1]

Department of Medicine, Division of Endocrinology, Diabetes, and Nutrition, University of Maryland School of Medicine, Baltimore, MD

Abstract **Hyperlipidemia and arterial cholesterol accumulation are primary causes of cardiovascular events. Monogenic forms of hyperlipidemia and recent genome-wide association studies indicate that genetics plays an important role. Zebrafish are a useful model for studying the genetic susceptibility to hyperlipidemia owing to conservation of many components of lipoprotein metabolism, including those related to LDL, ease of genetic manipulation, and in vivo observation of lipid transport and vascular calcification. We sought to develop a genetic model for lipid metabolism in zebrafish, capitalizing on one well-understood player in LDL cholesterol (LDL-c) transport, the LDL receptor (*ldlr*), and an established in vivo model of hypercholesterolemia. We report that morpholinos targeted against the gene encoding *ldlr* effectively suppressed its expression in embryos during the first 8 days of development. The *ldlr* morphants exhibited increased LDL-c levels that were exacerbated by feeding a high cholesterol diet. Increased LDL-c was ameliorated in morphants upon treatment with atorvastatin. Furthermore, we observed significant vascular and liver lipid accumulation, vascular leakage, and plaque oxidation in *ldlr*-deficient embryos. Finally, upon transcript analysis of several cholesterol-regulating genes, we observed changes similar to those seen in mammalian systems, suggesting that cholesterol regulation may be conserved in zebrafish. Taken together, these observations indicate conservation of *ldlr* function in zebrafish and demonstrate the utility of transient gene knockdown in embryos as a genetic model for hyperlipidemia.**—O'Hare, E. A., X. Wang, M. E. Montasser, Y-P. C. Chang, B. D. Mitchell, and N. A. Zaghloul. **Disruption of *ldlr* causes increased LDL-c and vascular lipid accumulation in a zebrafish model of hypercholesterolemia. *J. Lipid Res.* 2014.** 55: **2242–2253.**

Supplementary key words low density lipoprotein • low density lipoprotein receptor • atherosclerosis • low density lipoprotein cholesterol

Hypercholesterolemia is a primary cause of atherosclerosis and subsequent cardiovascular events. Genetic factors play a major role in regulation of plasma cholesterol levels, with heritability estimated to range from 40 to 70% [reviewed in (1)]. Over 100 genomic regions have been associated with changes in plasma lipid levels (2–5). Despite the large number of putative candidate genes identified, the functions of many remain largely unknown, owing in part to the lack of physiologically relevant in vivo models with which to validate and characterize the functionality of associated variants (3, 4, 6–13). Development of novel models in which genes can be individually targeted will likely reveal functional roles for genetic determinants of blood lipid levels and may facilitate discovery of novel targets for drug development.

The zebrafish is an excellent candidate for establishing genetic models of hyperlipidemia due to conservation of cell types and molecular pathways involved in lipid metabolism and cholesterol synthesis (8, 14–20). These include hepatocytes, adipocytes, and pancreatic acinar cells (17) as well as expression of genes involved in lipid transport and metabolism, such as LDL receptor (*ldlr*), sterol regulatory element binding protein (*srebp*) *1/2*, and HMG-CoA reductase (*Hmgcr*) (18–29). Consequently, mechanisms of lipid metabolism, storage, absorption, and transport are highly conserved in zebrafish, allowing for physiologically relevant investigation of these processes (20, 28, 30–34). Moreover, targeted suppression of gene expression can be easily achieved in zebrafish embryos, making assessment of the resulting larval phenotypes feasible for a large number

Support for this study was provided by National Institutes of Health Grants P30 DK072488, R01 HL121007 (B.D.M., Y-P.C.C., M.E.M., E.A.O., N.A.Z.), K01DK092402 (N.A.Z.), and T32-AG000219 (E.A.O.).

Manuscript received 20 December 2013 and in revised form 5 September 2014.

Published, JLR Papers in Press, September 8, 2014
DOI 10.1194/jlr.M046540

Abbreviations: CD, control diet; dpf, days postfertilization; *Hmgcr*, HMG-CoA reductase; hpf, hours postfertilization; *hsp70*, heat shock cognate 70 kD protein; LDL-c, LDL cholesterol; *ldlr*, LDL receptor; MO, morpholino; ORO, Oil Red O; OxLDL, oxidized LDL; *pcsk9*, proprotein convertase subtilisin/kexin type 9; qRT-PCR, quantitative RT-PCR; R5, repeat region 5; SB, splice-blocking; *srebp*, sterol regulatory element binding protein; TB, translation-blocking.

[1]To whom correspondence should be addressed.
e-mail: zaghloul@umaryland.edu

[S] The online version of this article (available at http://www.jlr.org) contains supplementary data in the form of seven figures.

Copyright © 2014 by the American Society for Biochemistry and Molecular Biology, Inc.

This article is available online at http://www.jlr.org

This is an Open Access article under the CC BY license.

of candidate genes. This is particularly useful in light of the recent development of a zebrafish model for diet-induced hypercholesterolemia characterized by elevated LDL cholesterol (LDL-c) levels and accumulation of vascular lipid deposits in larvae (35). A genetic model of hypercholesterolemia in zebrafish has not previously been reported, however. Here, we report the expansion of the zebrafish hypercholesterolemia model to include hypercholesterolemia as a result of genetic manipulation. The LDLR plays a well-understood role in LDL endocytosis, and mutations in the LDLR-encoding gene (*LDLR*) are associated with elevated plasma LDL-c levels and familial hypercholesterolemia (36–40). Our results demonstrate the feasibility of the zebrafish model through transient knockdown of the zebrafish homolog of LDLR, *ldlr*, by morpholino (MO), which resulted in hypercholesterolemia. These effects were significantly exacerbated when compounded with a high cholesterol diet (HCD) and were ameliorated by exogenous treatment with atorvastatin. Finally, we provide evidence that elevated LDL-c in *ldlr*-deficient larvae results in vascular and liver lipid accumulation, vascular leakage, increased plaque oxidation, macrophage recruitment, and hepatomegaly in larvae. Taken together, these data indicate conservation of *ldlr* function in zebrafish and support the use of this model to investigate genetic mechanisms of hypercholesterolemia.

MATERIALS AND METHODS

Zebrafish husbandry and embryo culture

Embryos were collected from natural matings of adult wild-type Tubingen zebrafish stocks maintained at 28.5°C. Embryos were cultured in embryo medium (41) at 28.5°C until harvesting at time points between 1 and 12 days postfertilization (dpf). All zebrafish procedures were approved by the University of Maryland Animal Care and Use Committee (protocol 0313013).

MO injection and validation

A splice-blocking (SB) MO (Gene Tools, LLC) was designed (5′-AGATCACATTTCATTTCTTACAGCA-3′) to target the intron 4-exon 4 splice junction of zebrafish *ldlr*. A translation-blocking (TB) MO was also used (5′-GATCTCCATAGTCTCTAAGCGAGCT-3′) to inhibit translation of zebrafish *ldlr*. Five nanograms of ldlr SB or TB MO, diluted in nuclease-free (DEPC-free) water containing 0.1% phenol red, was injected into one- or two-cell stage embryos. Five nanograms of nonspecific standard control MO (5′-CCTCTTACCTCAGTTACAATTTATA-3′) was used for control embryos. Embryos were injected with each MO and cultured at 28.5°C. Approximately 4,000 viable embryos were collected per MO per experiment for use in subsequent assays.

To validate disruption of splicing and removal of *ldlr* exon 4, cDNA was generated from *ldlr* (SB) and control morphants by isolation of whole embryo RNA and subsequent reverse transcription (RevertAid First Strand cDNA synthesis kit, Thermo Scientific) at each day of development starting at 24 h postfertilization (hpf) through 10 dpf. A total of 20 embryos were pooled for extraction of RNA at each time point. Experiments were repeated three times. Primers flanking *ldlr* exon 4 were designed with the following sequences: ldlr_SB_KD_forward primer, 5'-TGCAGACCCAGTCAGTTCAG-3'; ldlr_SB_KD_reverse primer, 5'-TCCATCTGGTAGCCATCCTC-3'.

To determine the nucleotides excised by the *ldlr* SB MO, PCR product generated using the same primers was sequenced using an Applied Biosystems model 3730XL 96-capillary high-throughput sequencer.

The *ldlr* normal and mutant (SB) cloning and transcript expression

Both the wild-type and aberrantly spliced *ldlr* transcripts were isolated from cDNA generated from zebrafish control and *ldlr* SB embryo homogenates, respectively. The open reading frame of each was amplified by PCR using the following primers: *ldlr*_gene_F, 5'-ATGGAGATCTCATTCATGCTTTTA-3'; *ldlr*_gene_R, 5'-TCATACCTGAGGGTAAAAATAGC-3'.

Products were gel-purified (QIAquick gel extraction kit) and cloned into the pCR2.1-TOPO TA vector (Life Technologies). Proper transcript length and sequence were confirmed via DNA sequencing. mRNA was transcribed from each construct using the mMESSAGE mMACHINE T7 transcription kit (Ambion) after linearization with *Sac*I. The *ldlr* mRNA was injected into embryos either alone or along with 5 ng *ldlr* SB MO.

Diets and feeding

Larvae (5 dpf) were fed either control diet (CD) [Zeigler AP100 (Aquatic Habitats, Inc.) + 10 μg/g BODIPY 576/589 C11 (Molecular Probes, Inc.)] or the same diet supplemented with 4% w/w cholesterol (HCD), as previously described (35). Diets were replaced twice daily until 7 dpf (48 h of feeding) or until 12 dpf (7 days of feeding).

LDL/VLDL cholesterol quantification

LDL-c levels were quantified from whole embryo homogenates consisting of 100 embryos per diet group homogenized in 400 μl of ice-cold 10 μM butylated hydroxytoluene. Homogenate was filtered through a 0.45 μm Dura PVDF membrane filter (Millipore) in preparation for lipid extraction and processed using the HDL and LDL/VLDL cholesterol assay kit (Cell Biolabs, Inc.) as per the manufacturer's protocol. After precipitation and dilution, samples were analyzed by fluorimetric analysis using a SpectraMax Gemini EM plate reader and SoftMax Pro microplate data acquisition and analysis software (Molecular Devices). Experiments were repeated at least three times. Values obtained by fluorimetric analysis were calculated relative to total protein concentration. Total protein was isolated from homogenates of 100 embryos in microcentrifuge tubes placed on ice after aspiration of embryo media and replacement with 500 μl cold RIPA buffer [150 mM NaCl, 1 mM EDTA, 50 mM Tris-HCl (pH 7.5), 1% NP-40] containing 1:100 protease inhibitor cocktail (Sigma P8340). After homogenization, tubes were rotated for 10 min at 4°C, then centrifuged at 12,000 *g* at 4°C for 10 min. Supernatant (20 μl) was transferred to a fresh tube and the protein concentration was quantified by BCA protein assay (Sigma C2284 and B9643).

Vascular lipid accumulation imaging and quantification

CD- or HCD-fed larvae were immobilized at 7 or 12 dpf by placement in one drop of 0.02% tricaine (Sigma-Aldrich) diluted in water on a glass depression microscope slide. Larvae were imaged at 20× magnification using an Olympus IX50 epifluorescent inverted microscope and cellSens Dimension software. The total number of BODIPY 576/589 C11-positive plaques was quantified in a 438.6 × 330.2 μm window along the caudal vein for a minimum of 25 larvae per MO per diet, as per published protocols (35, 42).

Quantitative RT-PCR

cDNA derived from mRNA isolated from pooled embryos (n = 20) of either *ldlr* SB or control morphants at 1–10 dpf were

used for quantification of gene expression using SYBR Green I (Roche). Samples and controls/standards were run in triplicates on a Roche LightCycler 480 instrument and mRNA expression levels were quantified relative to *β-actin*. Experiments were repeated at least three times. Primer sequences are available upon request.

Statin treatment

Embryo medium from CD- or HCD-fed larvae was removed after 24 h of feeding and replaced with atorvastatin-containing medium at a concentration of 50 μM (LKT Laboratories). Larvae were cultured at 28.5°C for an additional 24 h and then utilized in subsequent assays.

Oil Red O staining and liver size quantification

Larvae (5 and 7 dpf) were staged and fixed in 4% paraformaldehyde in PBS and incubated overnight at 4°C. Embryos were subsequently removed from the fixative and washed in 60% 2-propanol at room temperature; this was followed by a 3 h incubation in freshly filtered 0.3% Oil Red O (ORO) (Sigma, O0625) in 60% 2-propanol. To remove background staining prior to imaging, embryos were washed twice with 60% 2-propanol for 10 min and transferred to DEPC-treated water. Embryos were imaged using a Zeiss Lumar.V12 microscope and assessed for lipid density content. The size of the liver for ORO-stained control MOs (n = 20) and *ldlr* SB MO embryos (n = 20) at 4, 5, and 7 dpf was determined using ImageJ software.

LDLR antibody analysis, Western blot

Protein was extracted from pooled (n = 10) deyolked control MO-, *ldlr* SB MO-, and *ldlr* TB MO-injected embryos at 3, 5, and 7 dpf. Embryos were homogenized in 100 μl 2× SDS buffer [0.125 M Tris-Cl, 4% SDS, 20% v/v glycerol, 0.2 M DTT, 0.02% bromophenol blue, (pH 6.8)] and 2 μl protease inhibitor cocktail (Sigma) using a #23 syringe. PMSF (2 μl) was added and samples were then boiled for 5 min, cooled on ice for 5 min, and centrifuged for 3 min at 12,000 *g*. Ten microliters of each sample and protein ladder (Precision Plus Protein dual color standards #161-0374, Bio-Rad) were separated using 7.5% Criterion Tris-HCD gels (345-0007, Bio-Rad) at 100 V for 1 h. Proteins were transferred using a Criterion blotter (Bio-Rad) at 115 V for 1 h to Immobilon-P transfer membranes (IPVH00010, Millipore). The membranes were placed in blocking buffer for 1 h. The membranes were cut at 50 kDa in order to probe for both Ldlr (>50 kDa) and Actin (<50 kDa). The immunoblotting protocol was performed as follows: a 2 h room temperature incubation of anti-LDLR antibody (Sigma-Aldrich SAB3500286; 1:3,000) was followed by three 5 min washes using PBS/Tween; the secondary antibody, anti-chicken IgY (Sigma-Aldrich A9046; 1:160,000 dilution) was incubated for 2 h at room temperature followed by three PBS/Tween 15 min washes. Actin was detected by incubation with primary antibody (Sigma A2066; 1:3,000) for 2 h followed by secondary polyclonal goat anti-IgG antibody (Jackson ImmunoResearch Laboratories 111-035-003; 1:5,000). Chemiluminescence was enhanced using SuperSignal West Dura extended duration substrate (Thermo Scientific) following the manufacturer's protocol, and imaged using Alpha View-Fluor ChemQ software (Alpha Innotech Gel Imaging System for Life Science).

Identification of oxidized LDL plaques

Transgenic heat shock cognate 70 kDa protein (hsp70):IK17-eGFP zebrafish embryos (kindly received from Yury I. Miller, University of California, San Diego) were heat shocked for 1 h in a 37°C water bath prior to treatment with CD or HCD supplemented with cholesteryl BODIPY 576/589 at 5 dpf (42). At 7 dpf, embryos were immobilized by placement in one drop of 0.02% tricaine (Sigma-Aldrich) diluted in water on a glass depression microscope slide and imaged using an Olympus IX50 epifluorescent inverted microscope and cellSens Dimension software. Oxidized lipoprotein (OxLDL) was determined by colocalization of red BODIPY 576/589 and green IK17-eGFP. Experiments were repeated twice to confirm results and to obtain a total of 20 embryos per treatment.

Macrophage recruitment

HCD- or CD-fed embryos (7 dpf, control and morphant) were fixed in 10% neutral buffer formalin overnight and washed in PBS three times for 5 min prior to paraffin-embedding and collection of 10 μm thick transverse sections from 10 embryos per treatment group. Slides were washed three times in CitriSolv Hybrid (Decon Labs, Inc.) for 5 min each, followed by rehydration in 100, 95, 70, 50, and 25% ethanol (2 min each). Slides were then washed with PBS (5 min), treated in 0.1% Triton X-100 (5 min), and rewashed in PBS (5 min) prior to blocking (PBST, 1% BSA, 10% FBS) for 1 h at room temperature. Slides were immunostained using anti-human L-plastin (D-16) primary antibody (Santa Cruz Biotechnology sc-16657; 1:50) overnight in a humidity chamber at 4°C followed by two washes in PBS (5 min each) and 1 h incubation with Alexa Fluor® 594 donkey anti-goat IgG secondary antibody (Life Technologies A11058; 1:800), and 10 min counterstaining with DAPI (4′,6-diamidino-2-phenylindole) after two additional PBS washes (5 min each). Sections were imaged using an Olympus IX50 epifluorescent inverted microscope and cellSens Dimension software. To assess the colocalization of macrophages with cholesterol plaques, coverslips were removed by incubation at −20°C (25 min) followed by a PBS wash (5 min) and 10 min incubation with BODIPY 493/503 (Life Technologies; 1 mg/ml). Sections were washed again in PBS (5 min) and reimaged.

Vascular leakage

Larvae (7 dpf) were immobilized by anesthetization with 0.02% tricaine and placed in 0.3% methyl cellulose. Individual larvae were injected in the cardinal vein with 0.5 mg/ml dextran labeled with Alexa Fluor 594 (Life Technologies) as described in Stoletov et al. (35) followed by a wash with embryo medium and imaging 1 h after dextran injection. The presence of dextran was quantified at 10 μm from the caudal vein using ImageJ software. Signal intensity outside the lumen was normalized to signal intensity inside the lumen. Experiments were repeated at least twice.

Statistical analysis

Unless otherwise noted, a Student's *t*-test was used to determine significance. Bonferroni correction was used to adjust for multiple comparisons (at least four independent experiments in all cases).

RESULTS

MO injection disrupts *ldlr* expression through early development

Previous reports have demonstrated that zebrafish larvae become hypercholesteremic upon treatment with HCD, exhibiting increased total cholesterol and vascular plaques after 10 days of treatment (35, 42, 43). It is unknown, however, if hypercholesteremia in zebrafish can result from perturbation of gene expression. In humans,

loss-of-function mutations in *LDLR* are responsible for familial hypercholesterolemia (44, 45). To explore genetic hypercholesterolemia in zebrafish, we investigated the role of the zebrafish ldlr homolog (27). We first sought to determine the potential relevance of *ldlr* at larval stages by examining its expression starting at 1 dpf and at each day of development through 10 dpf. Endogenous *ldlr* could be detected by RT-PCR starting at 1 dpf and continued through 9 dpf (**Fig. 1A**). Quantification of *ldlr* transcript in control embryos by quantitative (q)RT-PCR revealed that expression at 1 dpf is low relative to *β-actin*, but continues to increase and is highly expressed by 9 dpf (Fig. 1A).

To determine a potential effect of loss of ldlr in zebrafish larvae, we targeted *ldlr* expression by MO injection. We designed a SB MO to target the intron 4-exon 4 splice junction of the unprocessed *ldlr* mRNA. To determine the efficacy of disruption of splicing, we also designed primers flanking the targeted splice junction which would amplify a 953 bp region of the wild-type mature mRNA. We first assessed the *ldlr* transcript at 1 dpf and found that only one band could be detected at approximately 950 bp in control MO-injected embryos (Fig. 1A). An additional band approximately 900 bp in length could also be detected in *ldlr* SB MO-injected embryos through 8 dpf (Fig. 1B), indicating the presence of an additional shorter transcript.

Targeting of the intron-exon splice junction of exon 4 could produce one of two possible outcomes. The first is exclusion of the entire exon 4 from the mature *ldlr* transcript as a result of disrupted splicing. However, exon 4 is 378 bp, and a mature mRNA lacking this exon should be 575 bp in length. Given that the PCR amplicon from the additional transcript is approximately 900 bp in length, a

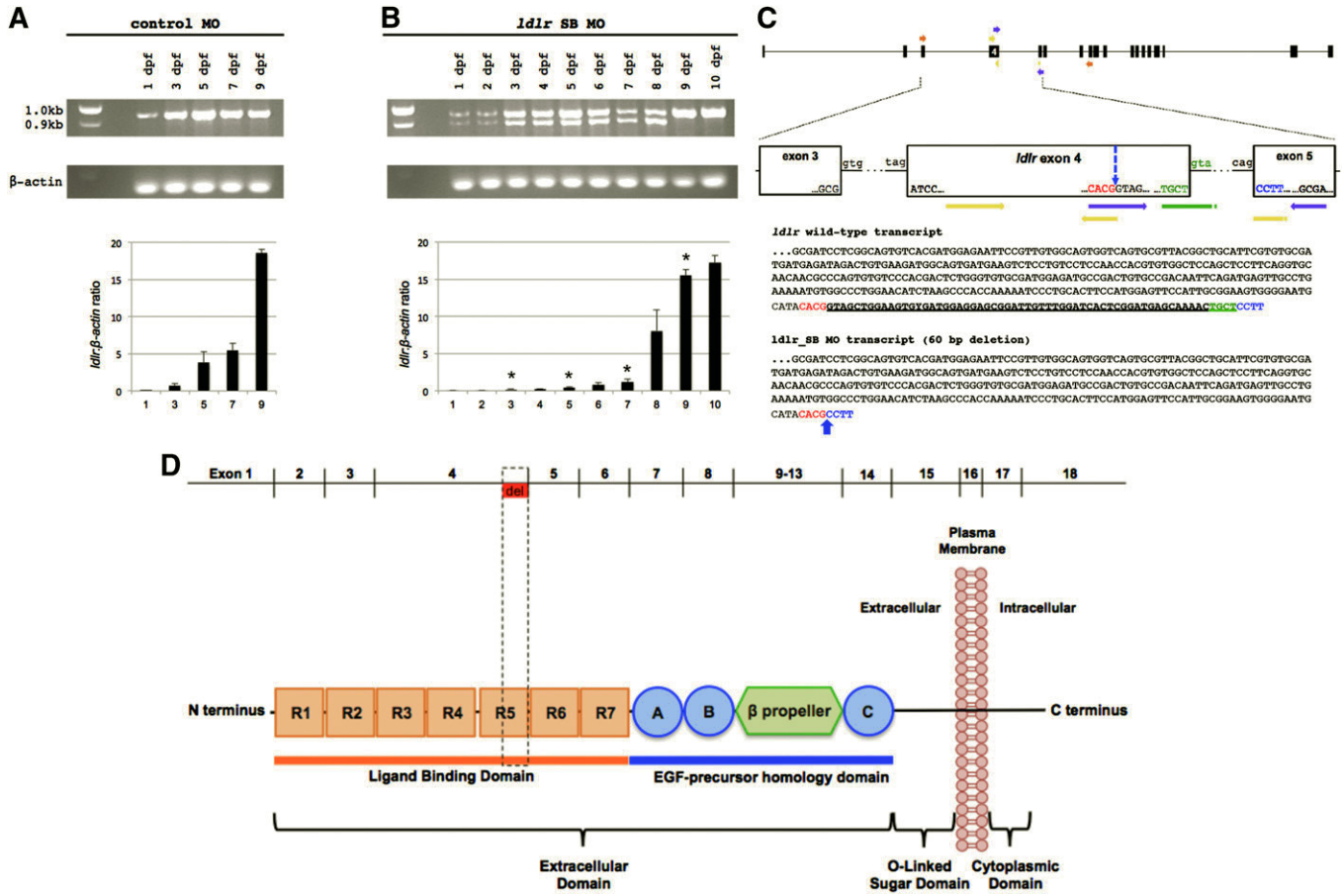

Fig. 1. Expression analysis identifies an aberrantly-spliced *ldlr* transcript in *ldlr* SB morphants. A: RT-PCR and qRT-PCR were performed on control embryos to determine endogenous *ldlr* expression levels from 1 dpf, at which point expression is low, through 9 dpf, when robust expression could be detected. B: RT-PCR amplification of a 953 bp region of the wild-type mature *ldlr* mRNA and a shorter (900 bp) aberrantly spliced transcript detectable until 8 dpf. qRT-PCR results from *ldlr* MO embryos at days 1–10 of development in which reduced expression was detected at days 1–7. $*P \leq 0.001$ relative to control after adjustment for multiple testing using Bonferroni correction. C: Sequence analysis of *ldlr* transcript isolated from MO-injected embryos indicated deletion of 60 nucleotides from exon 4. Orange arrows, forward and reverse *ldlr* MO knockdown validation primers; purple arrows, qRT-PCR primers to identify normal *ldlr* transcript; yellow arrows, qRT-PCR primers which span the spliced exon 4-exon 5 junction, used to identify *ldlr* SB morphant (−60 nt) transcript; green bar, *ldlr* SB targeted region; green text, *ldlr* SB MO targeted sequence; blue arrow, cryptic splice site; red text, nucleotides 5′ of spliced segment; blue text, nucleotides 3′ of splicing event representing the first four bases of exon 5; bold underlined text, deleted sequence by *ldlr* MO. D: Schematic of the mature *ldlr* mRNA (above) delineating exons and the corresponding domains (below). Red box indicates the 60 bp deleted region from the R5 ligand binding domain which is composed of seven 40-amino acid residue repeats (R) followed by the epidermal growth factor (EGF) precursor homology domain that contains three EGF-like repeats (A, B, and C in blue circles) and a β-propeller region.

difference of approximately 60 bp from the wild-type, a second outcome was considered: the creation of a cryptic splice site within exon 4 resulting in only partial removal of the exon. To evaluate this possibility, we sequenced the amplified region of the shorter transcript. Sequence analysis confirmed the absence of 60 nucleotides at the 3′ end of exon 4 in the *ldlr* SB MO-injected embryos (Fig. 1C). Interestingly, the removed region of the transcript corresponds to a partial loss of repeat region 5 (R5) in the ligand binding domain (Fig. 1D), a domain that is crucial for the function of mammalian LDLR (46–49). We characterized the effect of the exonic deletion by assessing the relative abundance of wild-type *ldlr* transcript in control and morphant embryos using primers that specifically detect it (Fig. 1C). At 1–7 dpf, a significant decrease in the level of wild-type *ldlr* transcript was detected, suggesting that the majority of *ldlr* transcript is targeted by the MO (Fig. 1A, B).

Increased LDL-c in *ldlr* morphants

Validation of MO efficacy through the first 7 days of development and the absence of gross morphological or developmental phenotypes (supplementary Fig. I) suggested the possibility of assessing other phenotypes beyond 5 dpf, when larvae begin to rely on exogenous sources of nutrients, including lipids, through feeding (20, 50, 51). Previous reports have indicated that treatment of 5 dpf larvae with a HCD resulted in elevated total cholesterol after 10 days of feeding, including evidence of increased LDL-c (35). To assess whether diet-induced changes in cholesterol could be produced by 7 dpf, we fed 5 dpf uninjected larvae with either CD or HCD twice daily for 2 days and measured LDL-c. LDL-c was significantly increased (P = 0.001) in HCD-fed larvae relative to CD-fed larvae by 7 dpf (supplementary Fig. II). Further, to verify the efficacy of our HCD treatment, we continued feeding until 12 dpf and observed significant ($P < 0.0001$) elevation of total LDL-c in those larvae (supplementary Fig. IIIA), corroborating previous studies (35, 43). Total protein was also assessed to ensure that any change in LDL-c levels was not a result of a change in protein concentration.

Increased LDL-c at 7 dpf implied the efficacy of HCD in raising cholesterol levels, even after a short treatment. We therefore asked whether suppression of *ldlr* by MO injection could impart similar effects at those stages when the MO is still effective. To test this, we fed control or *ldlr* morphants with either CD or HCD starting at 5 dpf for 48 h and assayed total LDL-c levels. Similar to uninjected embryos, LDL-c was significantly elevated to 14.6 μM in control MO-injected larvae treated with HCD relative to 11.6 μM in CD-fed larvae, representing a 26.5% increase (**Fig. 2A**; $P < 0.001$). Loss of *ldlr* expression exacerbated this effect. CD-fed *ldlr* MO-injected larvae exhibited increased LDL-c (13.9 μM), a significant increase relative to control morphants, suggesting hypercholesterolemia as a result of depleted *ldlr* alone ($P < 0.001$; Fig. 2A). The addition of HCD feeding to *ldlr* morphants resulted in a marked increase in LDL-c to 18.1 μM ($P < 0.001$; Fig. 2A).

Atorvastatin ameliorates hypercholesterolemia in zebrafish embryos

To further explore the conservation of cholesterol metabolism in zebrafish and the potential relevance to human hypercholesterolemia, we assessed a possible role for inhibition of *hmgcr* in regulation of total LDL-c in zebrafish larvae. In mammals, HMGCR catalyzes the rate-limiting step in de novo cholesterol synthesis and is targeted and inhibited by statins (52–56). The zebrafish homolog has been identified and mainly explored in the context of its role in migration of cells during development (57–61), though its potential to mediate cholesterol synthesis has been recently confirmed (62). To assess the possibility of LDL-c reduction by statin administration, we treated control or *ldlr* SB MO embryos, on either diet, with 50 μM

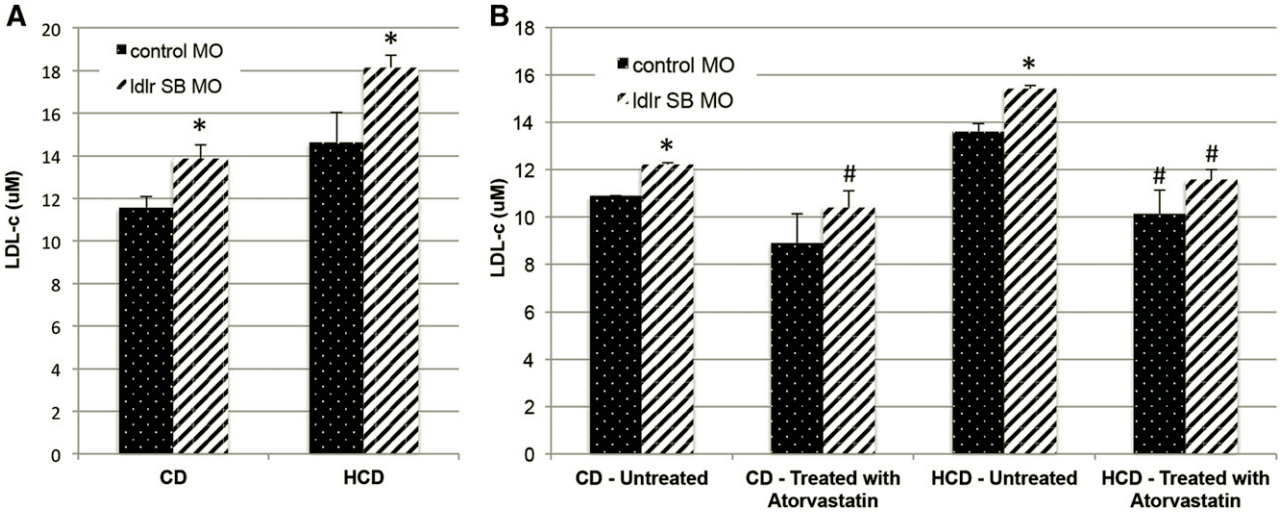

Fig. 2. LDL-c levels are altered in diet-fed and statin-treated morphants. A: LDL-c levels in 7 dpf control MO and *ldlr* SB MO subjected to either CD or HCD. B: LDL-c levels in CD- and HCD-fed control MO and *ldlr* SB MO embryos treated with atorvastatin for 24 h. *$P \leq 0.001$ relative to control after Bonferroni correction; #$P \leq 0.001$ relative to untreated embryos of the same MO injection group. LDL assay homogenates were comprised of 100 pooled embryos.

atorvastatin starting 24 h after initiation of feeding at 5 dpf; embryos were harvested 24 h later at 7 dpf. As expected, *ldlr* SB MO larvae on CD exhibited a significant increase in LDL-c relative to controls (Fig. 2B). Treatment with atorvastatin, however, significantly reduced this effect by 17.3%. Addition of the HCD also significantly increased LDL-c in both control and *ldlr* SB morphants, but these effects were reduced by 34.3 and 33.0%, respectively, upon treatment with atorvastatin ($P = 0.01$; Fig. 2B).

Increased vascular lipid accumulation in *ldlr* morphants

Hypercholesterolemic zebrafish larvae are susceptible to other pathogenic phenotypes, including vascular lipid accumulation and associated inflammation (35, 42, 43). Increased LDL-c in *ldlr* morphants suggests that these animals may be susceptible to similar consequences of increased circulating cholesterol. To test this possibility, we assessed the accumulation of cholesterol in the vasculature of *ldlr* morphants by supplementing either CD or HCD with cholesteryl BODIPY 576/589 C11, allowing for in vivo observation of cholesterol (35).

We imaged a 438.6 μm region of the posterior caudal vein where the majority of lipid deposits accumulate in hypercholesterolemic larvae (35) (**Fig. 3A, B**) and quantified the number of lipid plaques within the imaged region. At 7 dpf, control MO-injected embryos fed either a CD or HCD exhibited a very small number of vascular plaques on average, with many embryos exhibiting no observable lipid deposits (Fig. 3C, E, H). This is in contrast with previous reports describing plaque formation by 15 dpf, 10 days after initiation of HCD feeding (35). To verify the efficacy of the HCD treatment in generating vascular lipid accumulation, we extended HCD feeding to 12 dpf. In concordance with previous reports (35, 43), uninjected zebrafish subjected to either a CD or HCD for eight consecutive days exhibited plaque formation in the caudal vein (supplementary Fig. IIIB). Larvae fed HCD exhibited an approximate doubling of the average number of plaques, 3.5 plaques compared with 1.8 in CD-fed larvae, indicating the efficacy of the HCD diet in significantly increasing vascular lipid deposits over an extended period of feeding ($P = 0.002$; supplementary Fig. IIIB).

The resulting lipid accumulation in HCD-fed larvae over several days of feeding validated the presence of more severe phenotypes associated with elevated LDL-c. To determine whether suppression of *ldlr* expression could result in vascular lipid accumulation in zebrafish larvae, we cultured *ldlr* SB MO-injected embryos until 5 dpf and fed them with either a CD or HCD for 48 h. Strikingly, *ldlr* morphants fed either diet developed observable lipid deposits by 7 dpf. The *ldlr* morphant larvae treated with CD exhibited a significant increase in the average number of

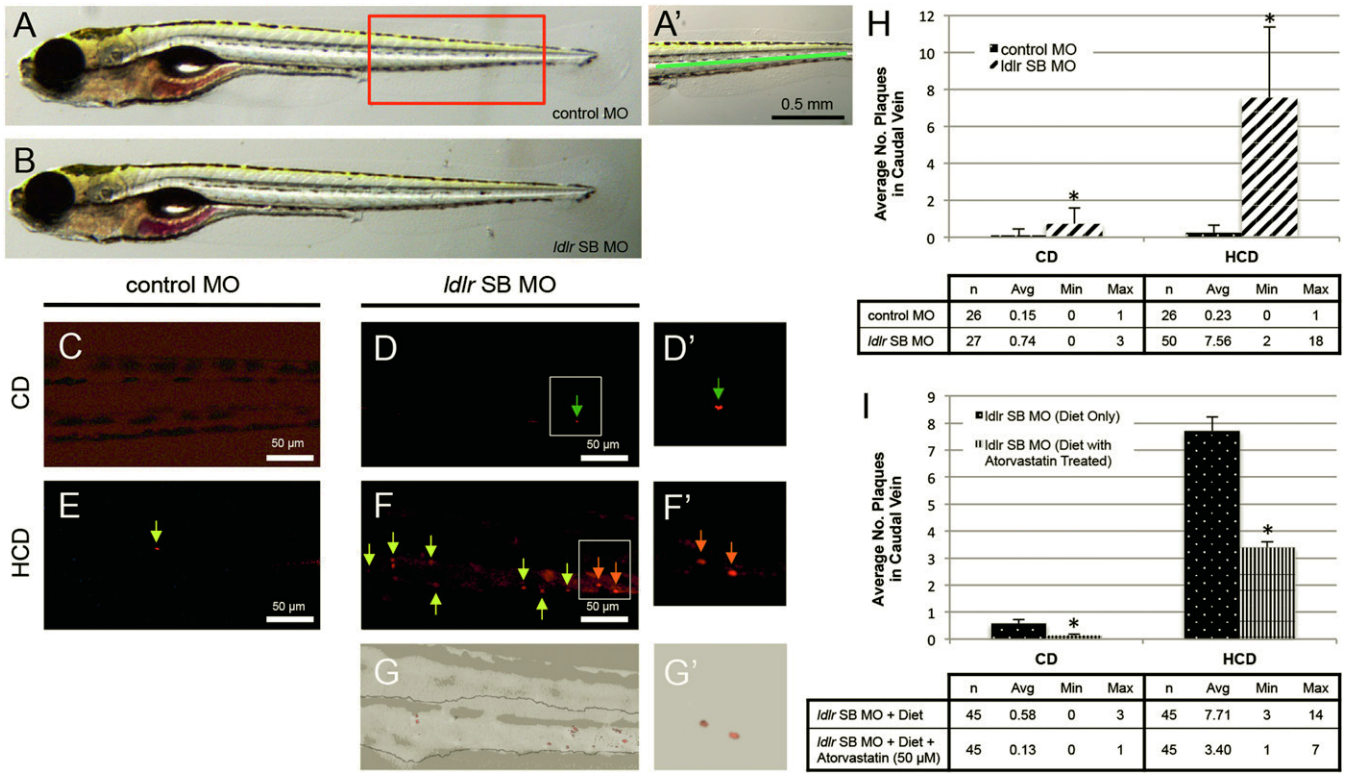

	n	Avg	Min	Max	n	Avg	Min	Max
control MO	26	0.15	0	1	26	0.23	0	1
ldlr SB MO	27	0.74	0	3	50	7.56	2	18

	n	Avg	Min	Max	n	Avg	Min	Max
ldlr SB MO + Diet	45	0.58	0	3	45	7.71	3	14
ldlr SB MO + Diet + Atorvastatin (50 μM)	45	0.13	0	1	45	3.40	1	7

Fig. 3. Cholesterol accumulation in vasculature of morphant zebrafish. A: Live control MO-injected embryo at 7 dpf. A': Location of assessment in the caudal vein; green line indicates region of plaque analysis. B: The *ldlr* SB morphant at 7 dpf. C–F': BODIPY-labeled cholesterol plaques (arrows) in control MO-injected embryo after 2 days of CD feeding (C) and *ldlr* SB morphants fed a CD (D). Control MO-injected embryo (E) and *ldlr* morphants fed a HCD (F). Boxed area magnified in (D') and (F'). G, G': Enhanced images of (F) and (F'). H: Quantification of the average number of plaques in control MO-injected and *ldlr* morphant embryos given either CD or HCD. I: Quantification of the average number of plaques in control MO-injected and *ldlr* morphant embryos given either CD or HCD and treated with 50 μM atorvastatin for 24 h. *$P \leq 0.001$ relative to control after Bonferroni correction.

vascular plaques relative to control MO-injected larvae ($P = 0.0006$; Fig. 3D, H), underscoring the severity of the hypercholesterolemic phenotype driven by loss of *ldlr* expression. Furthermore, *ldlr* morphants fed with HCD exhibited a 10-fold increase in the average number of vascular deposits relative to control embryos fed the same diet for the same period of time ($P < 0.0001$; Fig. 3F–H). We also assessed the effect of atorvastatin on plaque formation in *ldlr* SB morphants and found that in both CD-fed and HCD-fed *ldlr* SB morphants treatment with atorvastatin resulted in a significant decrease in plaque formation compared with their untreated counterparts (Fig. 3I). Taken together, these findings suggest that reduced *ldlr* expression results in more rapid and more severe onset of vascular lesions than those produced by diet alone.

Validation of *ldlr* MO effects

Our observations suggest that depletion of *ldlr* activity resulted in hypercholesterolemia and accumulation of vascular lipid deposits. We sought to validate that these defects were due to loss of *ldlr* specifically through two lines of evidence. First, we injected a second *ldlr* MO designed to disrupt translation of the protein (*ldlr* TB MO). Upon treatment with either diet, we observed increasing LDL-c levels as MO concentration increased, consistent with a dose-response and similar to *ldlr* SB MO (supplementary Fig. IVA). To verify the TB effects of the *ldlr* TB MO, we quantified Ldlr protein by Western blot. We observed a significant decrease in Ldlr through 7 dpf (supplementary Fig. IVB, C).

We next asked whether we could rescue the MO defects by coinjecting wild-type *ldlr* mRNA. Full-length wild-type *ldlr* open reading frame (ORF) was amplified from whole embryo cDNA and cloned into an expression vector for in vitro transcription. We coinjected wild-type *ldlr* mRNA with the *ldlr* SB MO and assessed plaque formation as well as LDL-c levels. We found that, whereas *ldlr* SB MO alone produced a significant increase in plaques and LDL-c, coinjection of *ldlr* mRNA reduced levels of both to be statistically indistinguishable from control MO (supplementary Fig. VA, B). Similarly, coinjection of wild-type mRNA rescued plaque formation and LDL-c in animals given HCD (supplementary Fig. VA, B). To verify that the 60 bp deletion produced by *ldlr* SB MO is deleterious, we generated *ldlr* mRNA harboring the deletion. Coinjection of this mRNA with the MO did not rescue LDL-c or plaque formation, supporting the loss of function imparted by the deletion (supplementary Fig. VA, B).

Expression of genes involved in cholesterol metabolism is perturbed in *ldlr* morphants

Several major genes regulate the expression of *ldlr*, thereby controlling lipid homeostasis in response to low intracellular cholesterol. These include *Srebp2*, which preferentially regulates cholesterol biosynthesis and uptake via transcriptional activation of *Hmgcr* and *Ldlr* (63, 64). Furthermore, expression of genes associated with HDL-c and removal of excess cholesterol is increased in response to elevated circulating cholesterol (65–70). To assess the response of genes associated with lipid homeostasis, we analyzed transcript levels in *ldlr* SB morphants. Expression of *srebp2*, *hmgcr*, and *abca1* were significantly increased relative to control animals, consistent with mammalian response (Supplementary Fig. VI). Interestingly, *pcsk9* levels were detected at very low levels in either control or *ldlr* SB MO-injected larvae, suggesting that this gene may be far less abundant or differentially regulated in zebrafish (supplementary Fig. VI).

LDL oxidation in *ldlr* morphants

The inflammatory response produced by OxLDL is the primary driver of atherosclerotic progression (71, 72). To assess the extent of LDL oxidation, we took advantage of a transgenic zebrafish line (hsp70:IK17-eGFP) expressing a functional single-chain antibody (scFv) of human IK17, tagged with GFP, under the control of the zebrafish *hsp70* promoter (42). Secreted IK17-eGFP binds to malondialdehyde epitopes on lipid deposits (OxLDL and malondialdehyde-LDL) in the vascular wall and activation of IK17-eGFP expression by heat shock results in the presence of GFP in oxidized plaques (42, 73). To determine whether OxLDL was present in the observed lesions in *ldlr* morphants, we injected MO into hsp70:IK17-eGFP embryos and fed either CD or HCD from 5–7dpf. Heat shock at 5 dpf for 1 h produced visible eGFP expression (**Fig. 4A, B**). On either diet, we observed a significant increase in colocalization of eGFP with BODIPY-labeled plaques in *ldlr* SB morphants (Fig. 4C–G).

To detect whether macrophages were recruited to the site of larval vascular lesions, we used a polyclonal antibody against human L-plastin, as previously described (35), to label macrophages in histological sections of HCD-fed *ldlr* morphants. Upon costaining with BODIPY 493/503, which labels neutral and other nonpolar lipids, we observed colocalization of L-plastin with lipid deposits within the vasculature (Fig. 4H–M).

Caudal vein vascular leakage in *ldlr* SB larvae

Hypercholesterolemia in both mice and zebrafish larvae results in the morphological disorganization and permeability of endothelial cells in the blood vessels (35, 74). The extent to which HCD affects the barrier function of the disorganized endothelial cell layer in zebrafish can be determined by injection of fluorescently labeled dextran directly into the circulation and assessment of dextran outside the lumen of the vasculature (35, 75). To determine the extent of vascular leakage in *ldlr* SB morphants fed CD or HCD, we injected *ldlr* SB morphants intravenously with dextran at 7 dpf and observed leakage outside the caudal vein. The presence of fluorescent dextran at 10 μm from the caudal vein lumen in *ldlr* SB morphants was approximately 2-fold higher in both CD- and HCD-fed larvae as compared with controls (**Fig. 5A–G**) suggesting disruption of vascular endothelium. Vascular leakage was reduced by 32% in HCD-fed controls and 56% in HCD-fed *ldlr* SB morphants by treatment with atorvastatin (Fig. 5G).

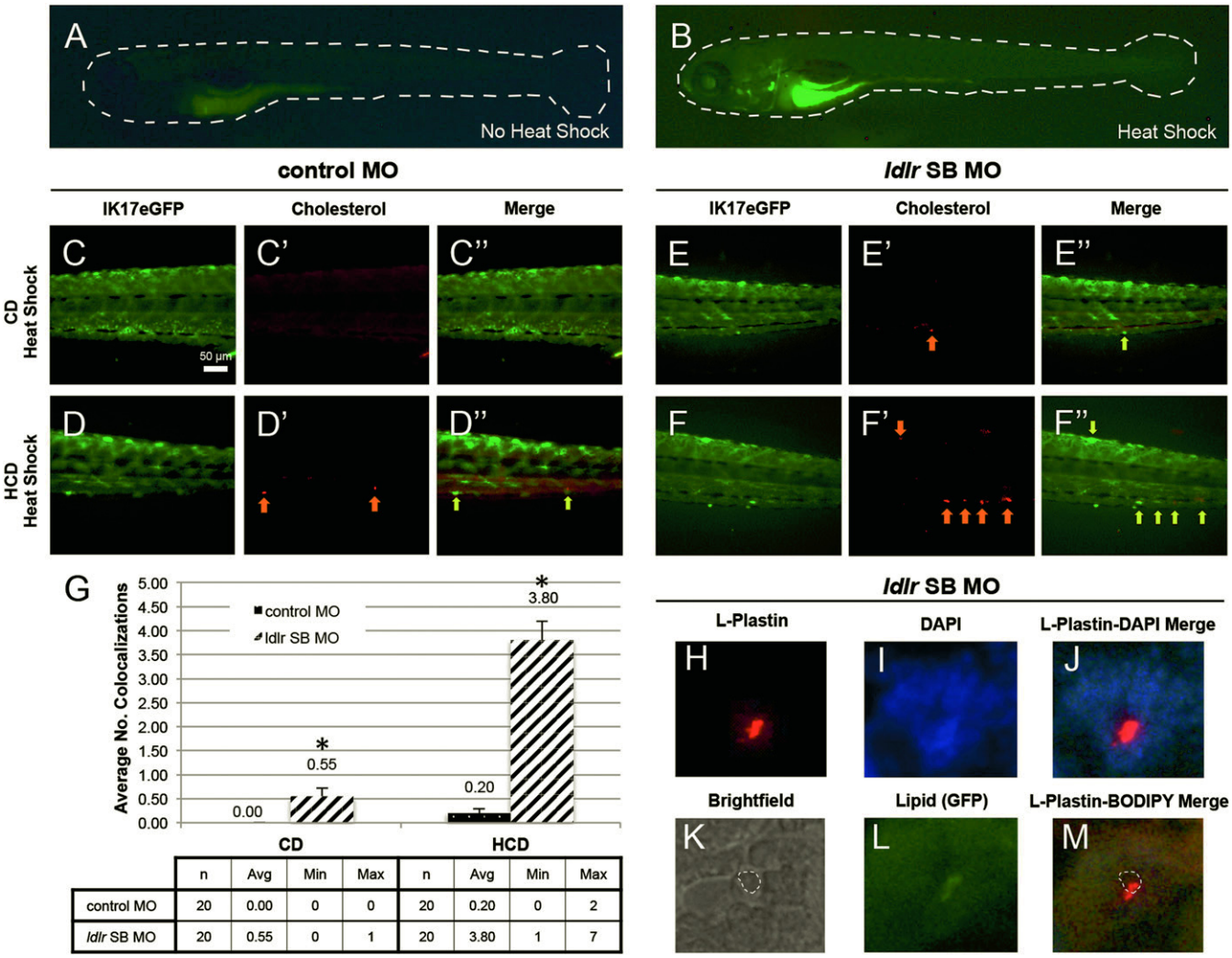

	CD n	CD Avg	CD Min	CD Max	HCD n	HCD Avg	HCD Min	HCD Max
control MO	20	0.00	0	0	20	0.20	0	2
ldlr SB MO	20	0.55	0	1	20	3.80	1	7

Fig. 4. The *ldlr* morphants exhibit more OxLDL-containing vascular plaques and macrophage infiltration. Transgenic hsp70:IK17-eGFP zebrafish embryos were subjected to 1 h of heat shock at 5 dpf and then fed a CD or HCD supplemented with fluorescent cholesteryl BODIPY 576/589 for 2 days. A, B: Only embryos that were heat shocked expressed eGFP fluorescence. Dashed line outlines the bodies of larvae. C, D: Control MO embryos fed a CD or HCD displayed no or little colocalization of green GFP and red BODIPY 576/589, but *ldlr* SB morphants fed a CD or HCD showed several colocalizations (E, F). G: Quantification of the average number of colocalizations (n = 20 total imaged per treatment). $*P \leq 0.001$ relative to control after Bonferroni correction. H–M: Representative paraffin section from *ldlr* SB morphant fed a HCD and immunostained with antibody against L-plastin (red) to identify the presence of macrophages. Colocalization was confirmed (J) in the vasculature (dashed line) near the dorsal aorta (K). L, M: Plaques were identified in histological sections using BODIPY 493/503 (green).

Increased liver lipid accumulation and hepatomegaly in *ldlr* morphants

Ldlr$^{-/-}$ mice, or those fed with diets high in cholesterol, exhibit accumulation of hepatic lipids (76, 77). To determine whether this was also true in zebrafish, we stained *ldlr* morphants using ORO. At 5 dpf, *ldlr* SB morphants exhibit hepatomegaly and increased accumulation of lipids in the liver, as compared with control MO larvae (supplementary Fig. VIIA–I). Liver size was also significantly increased in *ldlr* morphants after 48 h of either CD or HCD feeding (supplementary Fig. VIIB–F, I). Hepatic lipid content was significantly increased in *ldlr* morphants treated with CD (supplementary Fig. VIIB, E), though both controls and morphants accumulated hepatic lipid content when fed HCD (supplementary Fig. VIIC, F).

DISCUSSION

Loss-of-function mutations in LDLR are associated with hypercholesterolemia in humans and mice. Although *ldlr* has been identified in the zebrafish genome (27) and has an amino acid sequence identity to human *LDLR* of 56%, its manipulation to produce hypercholesteremia has not been demonstrated in zebrafish. Here, we report a model of elevated LDL-c as a result of depletion of zebrafish *ldlr*. Using transient knockdown by MO injection, we found that *ldlr* expression was suppressed through the first 8 days of development. This extended depletion of expression allowed for assessment of cholesterol phenotypes through development, including at and after stages when larvae begin exogenous feeding. Similar to mammalian models,

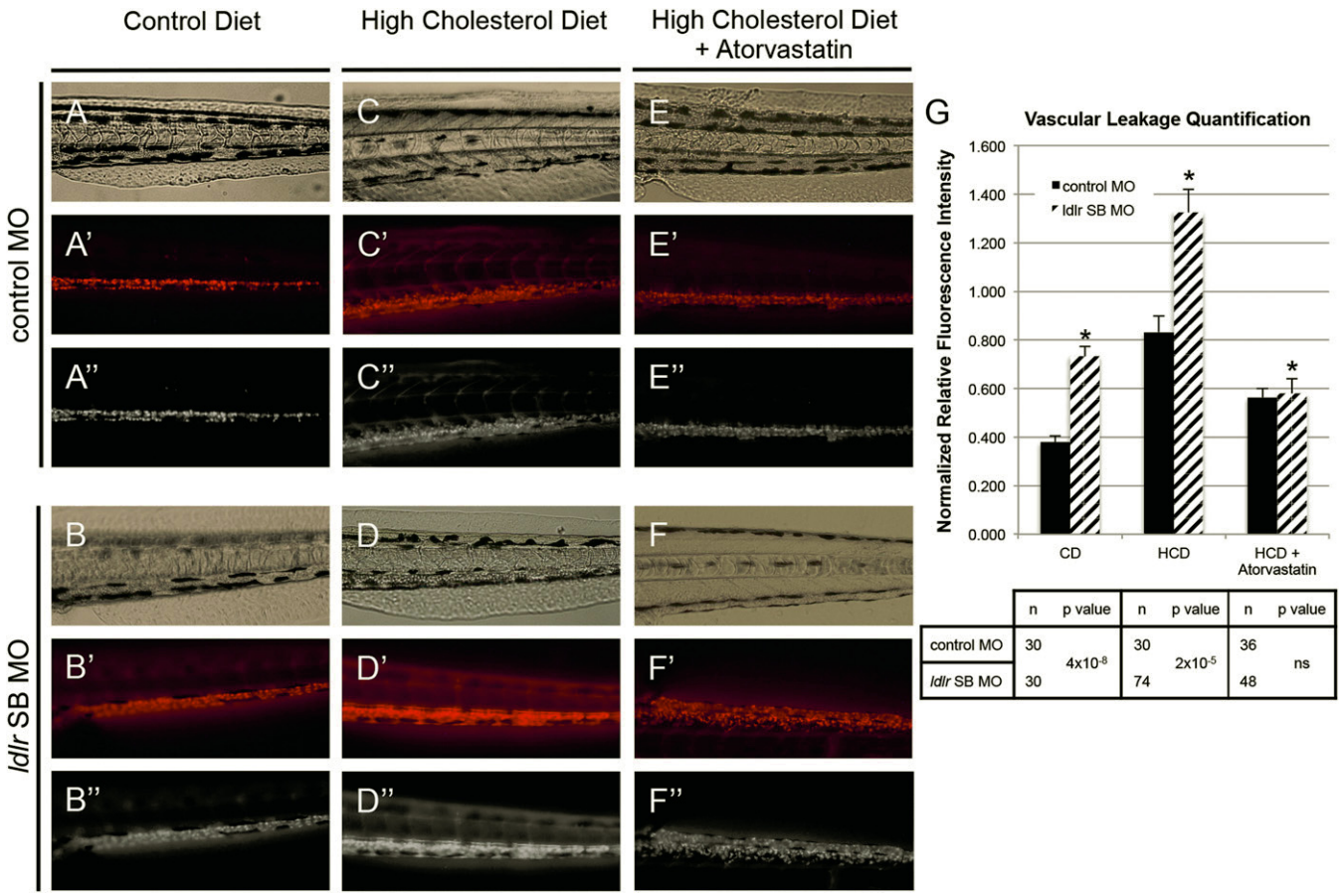

Fig. 5. Vascular leakage in *ldlr* SB morphants. A–F: Brightfield, fluorescent, and grayscale images of 7 dpf cardinal vein after injection with red fluorescent dextran and circulation for 1 h. G: Quantification of fluorescence intensity 10 μm away from the vascular lumen, quantified using ImageJ software. Embryos were individually assessed for vascular leakage. $*P \leq 0.01$ relative to control after Bonferroni correction.

we observed significantly elevated levels of LDL-c in larvae fed a CD, this effect was exacerbated by feeding of a HCD. Hypercholesterolemia was alleviated by treatment of larvae with atorvastatin. Furthermore, increased LDL-c was accompanied by changes in expression of genes regulating cholesterol homeostasis, *srebp2*, *hmgcr*, and *abca1*, vascular leakage, and hepatomegaly, as well as hepatic and vascular accumulation of oxidized cholesterol and macrophage infiltration. These findings suggest the conservation of Ldlr function in zebrafish, as well as conservation of pathways mediating both LDL- and HDL-c metabolism. Taken together, our data suggest the use of zebrafish as a model to investigate the functional relevance of genes to the regulation of LDL-c. Furthermore, our demonstration of the efficacy of transient knockdown in production of these phenotypes suggests the potential utility of this model for large-scale genetic investigation.

The relatively quick accumulation of LDL-c in larval zebrafish is in contrast with that observed in the mouse *Ldlr* knockout, in which plaques do not accumulate until approximately 3 months after introduction of increased dietary cholesterol (78, 79). The rapidity with which these changes occur may further broaden the appeal of using the zebrafish model to study the causes and consequences of hyperlipidemia. Furthermore, our findings suggest a conserved role for Ldlr in zebrafish which is consistent with other studies that have identified conservation of factors involved in lipid transport, such as caveolins, nuclear pore complex (NPC) proteins, and apolipoproteins (9, 33, 80). Indeed, the ortholog of the apoE protein, which LDLR recognizes on the surface VLDL/chylomicron particles (81, 82), has been identified and characterized in zebrafish (9). Though we did not investigate the extent to which Ldlr-apolipoprotein interaction was disrupted in our morphants, sequence confirmation of the partial removal of a ligand binding region of the receptor suggests a likely mechanism by which the MO disrupts Ldlr function. The exon targeted for deletion, exon 4, encompasses the ligand binding regions LR3–5, which are essential for mediating the interaction with lipoproteins (40, 49). Our MO resulted in removal of part of the R5 ligand binding domain which is essential for both apoB-100-mediated LDL binding and apoE-mediated lipoprotein binding (46, 48, 49, 83). Interestingly, over 50 mutations have been identified in familial hypercholesterolemia within this region of the human *LDLR* gene (40, 84–87).

Our study also suggests a conserved role for pathways that mediate Ldlr availability and cholesterol homeostasis, namely those mediated by *srebp2*. Though *pcsk9* expression was very low in either control or morphant larvae, its

expression was slightly decreased, though not significantly, in morphants. This suggests a possible differential mechanism of *pcsk9* regulation in zebrafish, though that remains to be determined. Increased expression of *srebp2* and *hmgcr*, however, implicate their responsiveness to intracellular LDL similar to the mammalian system (88). Increased circulating LDL-c as a result of impaired Ldlr function likely results in low intracellular levels of LDL, which in turn activate *srebp2* aimed at producing more LDLRs to increase uptake and more *hmgcr* to increase cholesterol synthesis [reviewed in (63, 89)]. Consistent with this, we observed increased expression of *srebp2* and *hmgcr* in *ldlr* morphants. This would potentially correlate with increased transcription of *ldlr*, though additional transcripts would likely continue to be targeted by the MO in our model. The yolk plays a critical role in lipid metabolism in early development (8, 50) and it is difficult to differentiate between changes that might affect the yolk, thereby affecting lipid traits in the embryo, compared with changes specific to experimental manipulation. It is important to note that, although we detected expression of *ldlr* at earlier stages when the yolk was still present, we did not assay cholesterol levels or induce dietary manipulations until after the stage at which the yolk was depleted and larvae began to feed.

Though CVD is a leading cause of death, relatively little is known about the contribution of genetic factors in common forms of the disease. In fact, over 100 genetic loci have been associated with cholesterol levels (2, 3), but the association signals often encompass multiple genes and the causal gene for each signal is not always clear. As our results demonstrate, larval zebrafish may offer a powerful tool both to validate the functional relevance of associated loci and to identify novel candidate genes. The combination of dietary manipulation (35) and genetic manipulation provides a robust platform with which to investigate multiple aspects of lipid metabolism and transport. Furthermore, the identification of pathogenic complications, including vascular lipid accumulation, oxidation, and macrophage infiltration (35, 42, 43), as well as obstruction of blood flow observed in our morphants (data not shown), suggests the utility of this model in understanding the progression of CVD.

REFERENCES

1. Dong, C., A. Beecham, L. Wang, S. Slifer, C. B. Wright, S. H. Blanton, T. Rundek, and R. L. Sacco. 2011. Genetic loci for blood lipid levels identified by linkage and association analyses in Caribbean Hispanics. *J. Lipid Res.* **52:** 1411–1419.
2. Willer, C. J. , E. M. Schmidt, S. Sengupta, G. M. Peloso, S. Gustafsson, S. Kanoni, A. Ganna, J. Chen, M. L. Buchkovich, S. Mora, et al.; Global Lipids Genetics Consortium. 2013. Discovery and refinement of loci associated with lipid levels. *Nat. Genet.* **45:** 1274–1283.
3. Teslovich, T. M., K. Musunuru, A. V. Smith, A. C. Edmondson, I. M. Stylianou, M. Koseki, J. P. Pirruccello, S. Ripatti, D. I. Chasman, C. J. Willer, et al. 2010. Biological, clinical and population relevance of 95 loci for blood lipids. *Nature.* **466:** 707–713.
4. Willer, C. J., and K. L. Mohlke. 2012. Finding genes and variants for lipid levels after genome-wide association analysis. *Curr. Opin. Lipidol.* **23:** 98–103.
5. Hegele, R. A. 2010. Genome-wide association studies of plasma lipids: have we reached the limit? *Arterioscler. Thromb. Vasc. Biol.* **30:** 2084–2086.
6. Rajan, A., and N. Perrimon. 2013. Of flies and men: insights on organismal metabolism from fruit flies. *BMC Biol.* **11:** 38.
7. Zhang, Y., X. Zou, Y. Ding, H. Wang, X. Wu, and B. Liang. 2013. Comparative genomics and functional study of lipid metabolic genes in Caenorhabditis elegans. *BMC Genomics.* **14:** 164.
8. Anderson, J. L., J. D. Carten, and S. A. Farber. 2011. Zebrafish lipid metabolism: from mediating early patterning to the metabolism of dietary fat and cholesterol. *In* The Zebrafish: Cellular and Developmental Biology, Part B. 3rd edition. H. W. Detrich III, M. Westerfield, and L. I. Zon, editors. Elsevier USA. 111–141.
9. Babin, P. J., C. Thisse, M. Durliat, M. Andre, M-A. Akimenko, and B. Thisse. 1997. Both apolipoprotein E and A-I genes are present in a nonmammalian vertebrate and are highly expressed during embryonic development. *Proc. Natl. Acad. Sci. USA.* **94:** 8622–8627.
10. Barter, P. J., H. B. Brewer, M. J. Chapman, C. H. Hennekens, D. J. Rader, and A. R. Tall. 2003. Cholesteryl ester transfer protein: a novel target for raising HDL and inhibiting atherosclerosis. *Arterioscler. Thromb. Vasc. Biol.* **23:** 160–167.
11. Kotokorpi, P., E. Ellis, P. Parini, L-M. Nilsson, S. Strom, K. R. Steffensen, J-Å. Gustafsson, and A. Mode. 2007. Physiological differences between human and rat primary hepatocytes in response to liver X receptor activation by 3-[3-[N-(2-chloro-3-trifluoromethylbenzyl)-(2,2-diphenylethyl)amino]propyloxy]phenylacetic acid hydrochloride (GW3965). *Mol. Pharmacol.* **72:** 947–955.
12. Wang, X., and B. Paigen. 2005. Genetics of variation in HDL cholesterol in humans and mice. *Circ. Res.* **96:** 27–42.
13. Bergen, W. G., and H. J. Mersmann. 2005. Comparative aspects of lipid metabolism: impact on contemporary research and use of animal models. *J. Nutr.* **135:** 2499–2502.
14. Lieschke, G. J., and P. D. Currie. 2007. Animal models of human disease: zebrafish swim into view. *Nat. Rev. Genet.* **8:** 353–367.
15. Pack, M., L. Solnica-Krezel, J. Malicki, S. C. Neuhauss, A. F. Schier, D. L. Stemple, W. Driever, and M. C. Fishman. 1996. Mutations affecting development of zebrafish digestive organs. *Development.* **123:** 321–328.
16. Schlegel, A., and D. Y. R. Stainier. 2006. Microsomal triglyceride transfer protein is required for yolk lipid utilization and absorption of dietary lipids in zebrafish larvae. *Biochemistry.* **45:** 15179–15187.
17. Wallace, K. N., S. Akhter, E. M. Smith, K. Lorent, and M. Pack. 2005. Intestinal growth and differentiation in zebrafish. *Mech. Dev.* **122:** 157–173.
18. Wallace, K. N., and M. Pack. 2003. Unique and conserved aspects of gut development in zebrafish. *Dev. Biol.* **255:** 12–29.
19. Walters, J. W., J. L. Anderson, R. Bittman, M. Pack, and S. A. Farber. 2012. Visualization of lipid metabolism in the zebrafish intestine reveals a relationship between NPC1L1-mediated cholesterol uptake and dietary fatty acid. *Chem. Biol.* **19:** 913–925. [Erratum. 2012. *Chem. Biol.* **19:** 1073.]
20. Hölttä-Vuori, M., V. T. V. Salo, L. Nyberg, C. Brackmann, A. Enejder, P. Panula, and E. Ikonen. 2010. Zebrafish: gaining popularity in lipid research. *Biochem. J.* **429:** 235–242.
21. Wallace, K. N., S. Yusuff, J. M. Sonntag, A. J. Chin, and M. Pack. 2001. Zebrafish hhex regulates liver development and digestive organ chirality. *genesis* 30: 141-143.
22. Yee, N. S., K. Lorent, and M. Pack. 2005. Exocrine pancreas development in zebrafish. *Dev. Biol.* **284:** 84–101.
23. Apelqvist, A., H. Li, L. Sommer, P. Beatus, D. J. Anderson, T. Honjo, M. H. de Angelis, U. Lendahl, and H. Edlund. 1999. Notch signalling controls pancreatic cell differentiation. *Nature.* **400:** 877–881.
24. Esni, F., B. Ghosh, A. V. Biankin, J. W. Lin, M. A. Albert, X. Yu, R. J. MacDonald, C. I. Civin, F. X. Real, M. A. Pack, et al. 2004. Notch inhibits Ptf1 function and acinar cell differentiation in developing mouse and zebrafish pancreas. *Development.* **131:** 4213–4224.
25. Zecchin, E., A. Mavropoulos, N. Devos, A. Filippi, N. Tiso, D. Meyer, B. Peers, M. Bortolussi, and F. Argenton. 2004. Evolutionary conserved role of ptf1a in the specification of exocrine pancreatic fates. *Dev. Biol.* **268:** 174–184.
26. Garcia-Calvo, M., J. Lisnock, H. G. Bull, B. E. Hawes, D. A. Burnett, M. P. Braun, J. H. Crona, H. R. Davis, D. C. Dean, P. A. Detmers, et al. 2005. The target of ezetimibe is Niemann-Pick C1-like 1 (NPC1L1). *Proc. Natl. Acad. Sci. USA.* **102:** 8132–8137.
27. Gregg, R. G., G. B. Willer, J. M. Fadool, J. E. Dowling, and B. A. Link. 2003. Positional cloning of the young mutation identifies an

essential role for the Brahma chromatin remodeling complex in mediating retinal cell differentiation. *Proc. Natl. Acad. Sci. USA.* **100:** 6535–6540.
28. Bauer, M. P., J. T. Bridgham, D. M. Langenau, A. L. Johnson, and F. W. Goetz. 2000. Conservation of steroidogenic acute regulatory (StAR) protein structure and expression in vertebrates. *Mol. Cell. Endocrinol.* **168:** 119–125.
29. Archer, A., S. Srinivas Kitambi, S. L. Hallgren, M. Pedrelli, K. Håkan Olsén, A. Mode, and J. Gustafsson. 2012. The liver X-receptor (Lxr) governs lipid homeostasis in zebrafish during development. *Open J. Endocr. Metab. Dis.* **2:** 74–81.
30. Clifton, J. D., E. Lucumi, M. C. Myers, A. Napper, K. Hama, S. A. Farber, A. B. Smith III, D. M. Huryn, S. L. Diamond, and M. Pack. 2010. Identification of novel inhibitors of dietary lipid absorption using zebrafish. *PLoS ONE.* **5:** e12386.
31. Marza, E., C. Barthe, M. André, L. Villeneuve, C. Hélou, and P. J. Babin. 2005. Developmental expression and nutritional regulation of a zebrafish gene homologous to mammalian microsomal triglyceride transfer protein large subunit. *Dev. Dyn.* **232:** 506–518.
32. Ho, S-Y., K. Lorent, M. Pack, and S. A. Farber. 2006. Zebrafish fat-free is required for intestinal lipid absorption and Golgi apparatus structure. *Cell Metab.* **3:** 289–300.
33. Nixon, S. J., J. Wegner, C. Ferguson, P-F. Méry, J. F. Hancock, P. D. Currie, B. Key, M. Westerfield, and R. G. Parton. 2005. Zebrafish as a model for caveolin-associated muscle disease; caveolin-3 is required for myofibril organization and muscle cell patterning. *Hum. Mol. Genet.* **14:** 1727–1743.
34. Annilo, T., Z-Q. Chen, S. Shulenin, J. Costantino, L. Thomas, H. Lou, S. Stefanov, and M. Dean. 2006. Evolution of the vertebrate ABC gene family: analysis of gene birth and death. *Genomics.* **88:** 1–11.
35. Stoletov, K., L. Fang, S-H. Choi, K. Hartvigsen, L. F. Hansen, C. Hall, J. Pattison, J. Juliano, E. R. Miller, F. Almazan, et al. 2009. Vascular lipid accumulation, lipoprotein oxidation, and macrophage lipid uptake in hypercholesterolemic zebrafish. *Circ. Res.* **104:** 952–960.
36. Goldstein, J. L., and M. S. Brown. 1992. Lipoprotein receptors and the control of plasma LDL cholesterol levels. *Eur. Heart J.* **13:** 34–36.
37. Goldstein, J. L., and M. S. Brown. 2009. The LDL receptor. *Arterioscler. Thromb. Vasc. Biol.* **29:** 431–438.
38. Hobbs, H. H., M. S. Brown, and J. L. Goldstein. 1992. Molecular genetics of the LDL receptor gene in familial hypercholesterolemia. *Hum. Mutat.* **1:** 445–466.
39. Varret, M., J. P. Rabes, and C. Boileau. 1997. Familial hypercholesterolemia 25 years after. 1. LDL receptor defects. *Med. Sci. (Paris).* **13:** 1399–1408.
40. Varret, M., and J-P. Rabés. 2012. Missense mutation in the LDLR gene: a wide spectrum in the severity of familial hypercholesterolemia. *In* Mutations in Human Genetic Disease. D. N. C. Cooper, editor. InTech, Rijeka, Croatia. 55–74.
41. Westerfield, M. 2000. The Zebrafish Book. A Guide for the Laboratory Use of Zebrafish (*Danio rerio*). 4th edition. University of Oregon Press, Eugene, OR.
42. Fang, L., S. R. Green, J. S. Baek, S-H. Lee, F. Ellett, E. Deer, G. J. Lieschke, J. L. Witztum, S. Tsimikas, and Y. I. Miller. 2011. In vivo visualization and attenuation of oxidized lipid accumulation in hypercholesterolemic zebrafish. *J. Clin. Invest.* **121:** 4861–4869.
43. Fang, L., R. Harkewicz, K. Hartvigsen, P. Wiesner, S-H. Choi, F. Almazan, J. Pattison, E. Deer, T. Sayaphupha, E. A. Dennis, et al. 2010. Oxidized cholesteryl esters and phospholipids in zebrafish larvae fed a high cholesterol diet: macrophage binding and activation. *J. Biol. Chem.* **285:** 32343–32351.
44. Hobbs, H. H., D. W. Russell, M. S. Brown, and J. L. Goldstein. 1990. The LDL receptor locus in familial hypercholesterolemia - mutational analysis of a membrane-protein. *Annu. Rev. Genet.* **24:** 133–170.
45. Tolleshaug, H., K. K. Hobgood, M. S. Brown, and J. L. Goldstein. 1983. The LDL receptor locus in familial hypercholesterolemia: Multiple mutations disrupt transport and processing of a membrane receptor. *Cell.* **32:** 941–951.
46. Nguyen, A. T., T. Hirama, V. Chauhan, R. MacKenzie, and R. Milne. 2006. Binding characteristics of a panel of monoclonal antibodies against the ligand binding domain of the human LDLr. *J. Lipid Res.* **47:** 1399–1405.
47. Kurasawa, J. H., S. A. Shestopal, E. Karnaukhova, E. B. Struble, T. K. Lee, and A. G. Sarafanov. 2013. Mapping the binding region on the low density lipoprotein receptor for blood coagulation factor VIII. *J. Biol. Chem.* **288:** 22033–22041.
48. Fisher, C., D. Abdul-Aziz, and S. C. Blacklow. 2004. A two-module region of the low-density lipoprotein receptor sufficient for formation of complexes with apolipoprotein E ligands. *Biochemistry.* **43:** 1037–1044.
49. Russell, D. W., M. S. Brown, and J. L. Goldstein. 1989. Different combinations of cysteine-rich repeats mediate binding of low-density lipoprotein receptor to 2 different proteins. *J. Biol. Chem.* **264:** 21682–21688.
50. Jones, K. S., A. P. Alimov, H. L. Rilo, R. J. Jandacek, L. A. Woollett, and W. T. Penberthy. 2008. A high throughput live transparent animal bioassay to identify non-toxic small molecules or genes that regulate vertebrate fat metabolism for obesity drug development. *Nutr. Metab. (Lond).* **5:** 23.
51. Anderson, J. L., J. D. Carten, and S. A. Farber. 2011. Zebrafish lipid metabolism: from mediating early patterning to the metabolism of dietary fat and cholesterol. *Methods Cell Biol.* **101:** 111–141.
52. Osborne, T. F., J. L. Goldstein, and M. S. Brown. 1985. 5′ end of HMG CoA reductase gene contains sequences responsible for cholesterol-mediated inhibition of transcription. *Cell.* **42:** 203–212.
53. Luskey, K. L., and B. Stevens. 1985. Human 3-hydroxy-3-methylglutaryl coenzyme A reductase. Conserved domains responsible for catalytic activity and sterol-regulated degradation. *J. Biol. Chem.* **260:** 10271–10277.
54. Brown, M. S., and J. L. Goldstein. 1980. Multivalent feedback regulation of HMG CoA reductase, a control mechanism coordinating isoprenoid synthesis and cell growth. *J. Lipid Res.* **21:** 505–517.
55. Istvan, E. S., and J. Deisenhofer. 2001. Structural mechanism for statin inhibition of HMG-CoA reductase. *Science.* **292:** 1160–1164.
56. Endo, A. 1992. The discovery and development of HMG-CoA reductase inhibitors. *J. Lipid Res.* **33:** 1569–1582.
57. Santos, A. C., and R. Lehmann. 2004. Isoprenoids control germ cell migration downstream of HMGCoA Reductase. *Dev. Cell.* **6:** 283–293.
58. Thorpe, J. L., M. Doitsidou, S-Y. Ho, E. Raz, and S. A. Farber. 2004. Germ cell migration in zebrafish is dependent on HMGCoA reductase activity and prenylation. *Dev. Cell.* **6:** 295–302.
59. Choi, J., K. Mouillesseaux, Z. Wang, H. D. G. Fiji, S. S. Kinderman, G. W. Otto, R. Geisler, O. Kwon, and J-N. Chen. 2011. Aplexone targets the HMG-CoA reductase pathway and differentially regulates arteriovenous angiogenesis. *Development.* **138:** 1173–1181.
60. D'Amico, L., I. C. Scott, B. Jungblut, and D. Y. R. Stainier. 2007. A mutation in zebrafish hmgcr1b reveals a role for isoprenoids in vertebrate heart-tube formation. *Curr. Biol.* **17:** 252–259.
61. Mapp, O. M., G. S. Walsh, C. B. Moens, M. Tada, and V. E. Prince. 2011. Zebrafish Prickle1b mediates facial branchiomotor neuron migration via a farnesylation-dependent nuclear activity. *Development.* **138:** 2121–2132.
62. Eisa-Beygi, S., G. Hatch, S. Noble, M. Ekker, and T. W. Moon. 2013. The 3-hydroxy-3-methylglutaryl-CoA reductase (HMGCR) pathway regulates developmental cerebral-vascular stability via prenylation-dependent signalling pathway. *Dev. Biol.* **373:** 258–266.
63. Brown, M. S., and J. L. Goldstein. 1997. The SREBP pathway: regulation of cholesterol metabolism by proteolysis of a membrane-bound transcription factor. *Cell.* **89:** 331–340.
64. Horton, J. D., J. L. Goldstein, and M. S. Brown. 2002. SREBPs: activators of the complete program of cholesterol and fatty acid synthesis in the liver. *J. Clin. Invest.* **109:** 1125–1131.
65. Clarke, R., C. Frost, R. Collins, P. Appleby, and R. Peto. 1997. Dietary lipids and blood cholesterol: Quantitative meta-analysis of metabolic ward studies. *BMJ.* **314:** 112–117.
66. Howell, W. H., D. J. McNamara, M. A. Tosca, B. T. Smith, and J. A. Gaines. 1997. Plasma lipid and lipoprotein responses to dietary fat and cholesterol: A meta-analysis. *Am. J. Clin. Nutr.* **65:** 1747–1764.
67. Walden, C. E., B. M. Retzlaff, B. L. Buck, S. Wallick, B. S. McCann, and R. H. Knopp. 2000. Differential effect of National Cholesterol Education Program (NCEP) Step II diet on HDL cholesterol, its subfractions, and apoprotein A-I levels in hypercholesterolemic women and men after 1 year: the beFIT study. *Arterioscler. Thromb. Vasc. Biol.* **20:** 1580–1587.
68. Tall, A. R. 1990. Plasma high-density lipoproteins. Metabolism and relationship to atherogenesis. *J. Clin. Invest.* **86:** 379–384.
69. Gatto, L. M., M. A. Lyons, A. J. Brown, and S. Samman. 2001. Trans fatty acids and cholesterol metabolism: mechanistic studies in rats and rabbits fed semipurified diets. *Int. J. Food Sci. Nutr.* **52:** 435–441.

70. Krieger, M. 1999. Charting the fate of the "good cholesterol": identification and characterization of the high-density lipoprotein receptor SR-BI. *Annu. Rev. Biochem.* **68:** 523–558.
71. Glass, C. K., and J. L. Witztum. 2001. Atherosclerosis: the road ahead. *Cell.* **104:** 503–516.
72. Itabe, H., T. Obama, and R. Kato. 2011. The dynamics of oxidized LDL during atherogenesis. *J. Lipids.* **2011:** 418313.
73. Shaw, P. X., S. Hörkkö, S. Tsimikas, M-K. Chang, W. Palinski, G. J. Silverman, P. P. Chen, and J. L. Witztum. 2001. Human-derived anti-oxidized LDL autoantibody blocks uptake of oxidized LDL by macrophages and localizes to atherosclerotic lesions in vivo. *Arterioscler. Thromb. Vasc. Biol.* **21:** 1333–1339.
74. Mullick, A. E., K. Soldau, W. B. Kiosses, T. A. Bell III, P. S. Tobias, and L. K. Curtiss. 2008. Increased endothelial expression of Toll-like receptor 2 at sites of disturbed blood flow exacerbates early atherogenic events. *J. Exp. Med.* **205:** 373–383.
75. Stoletov, K., V. Montel, R. D. Lester, S. L. Gonias, and R. Klemke. 2007. High-resolution imaging of the dynamic tumor cell–vascular interface in transparent zebrafish. *Proc. Natl. Acad. Sci. USA.* **104:** 17406–17411.
76. Subramanian, S., L. Goodspeed, S. Wang, J. Kim, L. Zeng, G. N. Ioannou, W. G. Haigh, M. M. Yeh, K. V. Kowdley, K. D. O'Brien, et al. 2011. Dietary cholesterol exacerbates hepatic steatosis and inflammation in obese LDL receptor-deficient mice. *J. Lipid Res.* **52:** 1626–1635.
77. Bieghs, V., F. Verheyen, P. J. van Gorp, T. Hendrikx, K. Wouters, D. Luetjohann, M. J. J. Gijbels, M. Febbraio, C. J. Binder, M. H. Hofker, et al. 2012. Internalization of modified lipids by CD36 and SR-A leads to hepatic inflammation and lysosomal cholesterol storage in Kupffer cells. *PLoS ONE.* **7:** e34378.
78. Lichtman, A. H., S. K. Clinton, K. Iiyama, P. W. Connelly, P. Libby, and M. I. Cybulsky. 1999. Hyperlipidemia and atherosclerotic lesion development in LDL receptor-deficient mice fed defined semipurified diets with and without cholate. *Arterioscler. Thromb. Vasc. Biol.* **19:** 1938–1944.
79. Ma, Y., W. Wang, J. Zhang, Y. Lu, W. Wu, H. Yan, and Y. Wang. 2012. Hyperlipidemia and atherosclerotic lesion development in Ldlr-deficient mice on a long-term high-fat diet. *PLoS ONE.* **7:** e35835.
80. van der Meer, D. L. M., G. E. E. J. M. van den Thillart, F. Witte, M. A. G. de Bakker, J. Besser, M. K. Richardson, H. P. Spaink, J. T. D. Leito, and C. P. Bagowski. 2005. Gene expression profiling of the long-term adaptive response to hypoxia in the gills of adult zebrafish. *Am. J. Physiol. Regul. Integr. Comp. Physiol.* **289:** R1512–R1519.
81. Olofsson, S-O., O. Wiklund, and J. Boren. 2007. Apolipoproteins A-I and B: biosynthesis, role in the development of atherosclerosis and targets for intervention against cardiovascular disease. *Vasc. Health Risk Manag.* **3:** 491–502.
82. Brown, M. S., and J. L. Goldstein. 1986. A receptor-mediated pathway for cholesterol homeostasis. *Science.* **232:** 34–47.
83. Mahley, R. W., T. L. Innerarity, K. H. Weisgraber, and D. L. Fry. 1977. Canine hyperlipoproteinemia and atherosclerosis. Accumulation of lipid by aortic medial cells in vivo and in vitro. *Am. J. Pathol.* **87:** 205–226.
84. Neff, D., F. Ruschitzka, M. Hersberger, F. Enseleit, D. Hurlimann, G. Noll, T. Luscher, and E. Hanseler. 2003. Detection of a novel exon 4 low-density lipoprotein receptor gene deletion in a Swiss family with severe familial hypercholesterolemia. *Clin. Chem. Lab. Med.* **41:** 266–271.
85. Theart, L., M. J. Kotze, E. Langenhoven, O. Loubser, A. V. Peeters, C. J. Lintott, and R. S. Scott. 1995. Screening for mutations in exon-4 of the LDL receptor gene: identification of a new deletion mutation. *J. Med. Genet.* **32:** 379–382.
86. Goldmann, R., L. Tichy, T. Freiberger, P. Zapletalova, O. Letocha, V. Soska, J. Fajkus, and L. Fajkusova. 2010. Genomic characterization of large rearrangements of the LDLR gene in Czech patients with familial hypercholesterolemia. *BMC Med. Genet.* **11:** 115.
87. Chmara, M., B. Wasag, M. Zuk, J. Kubalska, A. Wegrzyn, M. Bednarska-Makaruk, E. Pronicka, H. Wehr, J. C. Defesche, A. Rynkiewicz, et al. 2010. Molecular characterization of Polish patients with familial hypercholesterolemia: novel and recurrent LDLR mutations. *J. Appl. Genet.* **51:** 95–106.
88. Hart, L. M., P. de Knijff, J. M. Dekker, R. P. Stolk, G. Nijpels, F. E. van der Does, J. B. Ruige, D. E. Grobbee, R. J. Heine, and J. A. Maassen. 1999. Variants in the sulphonylurea receptor gene: association of the exon 16-3t variant with type II diabetes mellitus in Dutch Caucasians. *Diabetologia.* **42:** 617–620.
89. Llorente-Cortés, V., P. Costales, J. Bernués, S. Camino-Lopez, and L. Badimon. 2006. Sterol regulatory element-binding protein-2 negatively regulates low density lipoprotein receptor-related protein transcription. *J. Mol. Biol.* **359:** 950–960.